The Onset and Early Growth of Snow Crystals by Accretion of Droplets[1]

ROGER F. REINKING

Boundary Layer Dynamics Group, Weather Modification Program Office, Environmental Research Laboratories/NOAA, Boulder, CO 80303

(Manuscript received 26 September 1978, in final form 6 February 1979)

ABSTRACT

Snow crystals sampled from winter storms of the Sierra Nevada have been examined to determine their riming characteristics in terms of their dimensions and habits of growth. The field data show that accretion can begin on crystals that have grown for only 2–4 min. However, the onset of accretion is delayed over longer growth periods for many crystals, so considerable dispersion occurs in the size at the onset of riming on specific types of crystals. This dispersion, which occurs in individual snow showers as well as over the durations of whole storms, and results from interactions of various cloud processes, is very important in describing and modeling snow crystal growth.

The minimum sizes of the observed crystals at the onset of accretion, in terms of major crystal dimensions, ranged from 115 to 320 μm. The minimum widths of different columnar types at the onset were very uniform (30–36 μm). Nevertheless, the basic columnar and planar habits show very systematic differences in minimum dimensions and durations of growth required for riming to begin; the measured sizes and growth times are somewhat less than those predicted by the more rigid of the current theories of accretion.

The systematic differences among the various habits carry through to heavier stages of accretion. Individually branched planar and radiating crystals and capped columns develop the highest rates of accretion and precipitate the most water in the form of rime. Total precipitation, of course, depends on the concentrations of the various crystals. Assuming that the laboratory evidence for the rime-droplet splintering mechanism can be applied in the field, significant needle and sheath production through such multiplication probably occurred in the Sierran cloud systems.

1. Introduction

Snow crystals can accrete mass by collecting and freezing supercooled cloud droplets. The growth of snow crystals by this riming process begins after crystal growth by vapor deposition has progressed for some time. The time elapsed between nucleation of an ice crystal and the onset of droplet accretion is dependent on crystal size and habit of growth, and on the presence and size distribution of supercooled droplets in the cloud. A number of microphysical and dynamical processes interact to cause or prevent accretion, to determine the effects crystal riming will have on other cloud processes, to regulate the rate and final amount of rime accreted on the crystals that populate a mixed-phase cloud, and thus to influence the water budget of the cloud. Some of these process interactions are shown schematically in the flow chart of Fig. 1. This schematic is by no means all inclusive, but does show the principal routes from ice crystal nucleation to precipitation.

As indicated in the figure, the onset of accretion and the continuation of riming depend on the rate of droplet condensation and the competing rate of vapor deposition on the crystals. The accumulation of significant rime can increase crystal fallspeed, ventilation and the rate of deposition, and further influences the crystal trajectory, the rate of new riming and the in-cloud residence time. The onset of riming may signal the start of secondary ice particle production, possibly by droplet splintering (Hallett and Mossop, 1974; Mason, 1975). The quantities of secondary ice particles produced may be regulated by the accretion rate and, therefore, by the duration of crystal growth required to accumulate significant rime. Jiusto and Lavoie (1975) have concluded that "the riming concept and its further refinement should rank high on or head the priority list for (studies to explain) ice multiplication," and "the critical size and time for riming onset must be considered."

In this paper, the onset and early stages of riming of snow crystals are described from field measurements. The study is based on snow crystal data collected during winter storms of the central Sierra Nevada. Riming of snow crystals with each of the basic growth habits is investigated. Results from these field data are compared with theoretical findings and other empirical results.

[1] Based on work done while author was at the Naval Weapons Center, China Lake, CA.

Unauthenticated | Downloaded 05/21/24 01:11 AM UTC

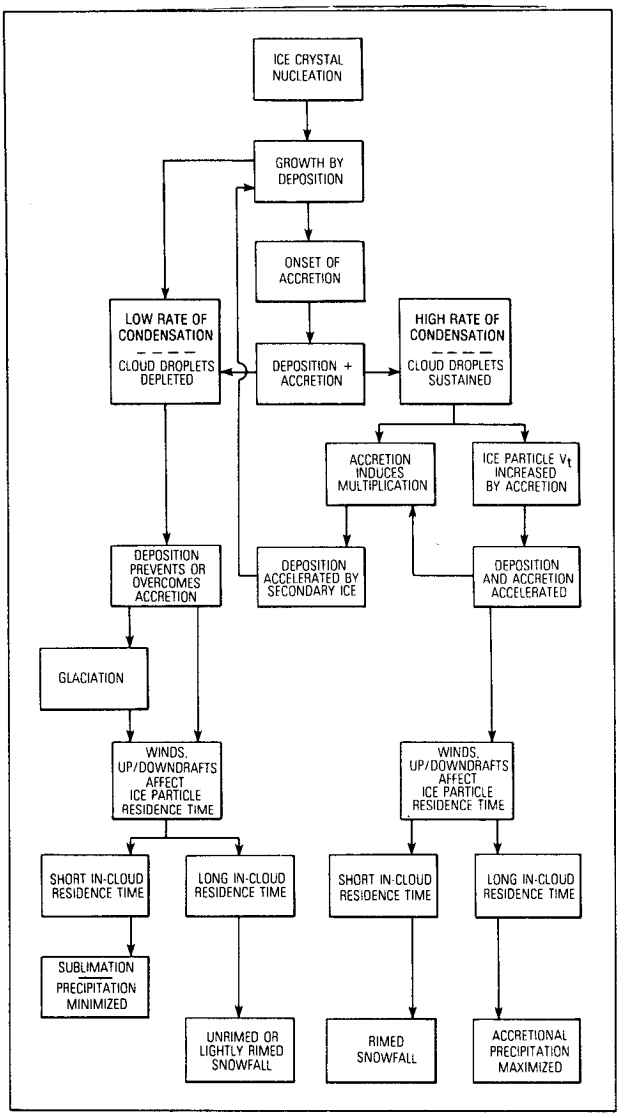

FIG. 1. Principal interactions of accretion with other microphysical and dynamical cloud processes.

2. Data and methods

The data for this study were collected during the field weather modification experiments of the Bureau of Reclamation Project CENSARE (CENtral SierrA REsearch). The project was designed to study snow generating processes and the corresponding potential for enhancing precipitation by cloud seeding. Some 14 500 snow crystals were analyzed from 260 individual samples collected during nine synoptically diverse Sierra Nevada snowstorms of the 1971–72 and 1972–73 seasons. Eight storms were seeded, one was not. The crystal sampling site was at Tamarack, California (2109 m MSL), on the western slope of the Sierra Nevada near the mean elevation of maximum snowfall. The ice particles were replicated in plastic at 15–45 min intervals during snowfall. Analyses here are primarily

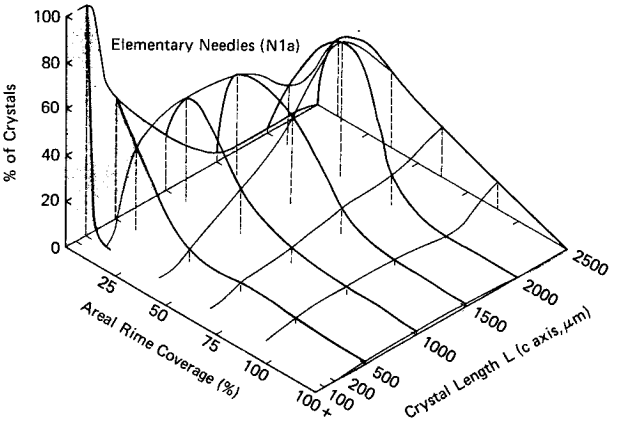

FIG. 2. Frequency distribution of the amounts of accretion (areal rime coverage) on elementary needles, in terms of snow crystal length. Size intervals used in plotting are specified by their midpoints on this and following graphs. Narrower size intervals were plotted for the smallest crystal lengths than for the larger lengths to enhance illustration of the early riming (e.g., 100 μm represents the 50–150 μm interval, whereas 500 μm represents the 250–750 μm interval).

for the seeded storms, which contributed 96.6% of the crystals sampled.

Background and details of the data analysis methods are given by Reinking (1973, 1975). Briefly, they are as follows.

Crystal axes were measured, and growth habits were identified from the replicas according to the classification of Magono and Lee (1966). The various types of crystals observed, designations of major groups and corresponding sample sizes are given in Table 1 of Reinking (1975) and, with corresponding formation temperatures, in Reinking (1973). As also explained in these references, the varied amounts of rime on individual crystals were measured to describe the onset

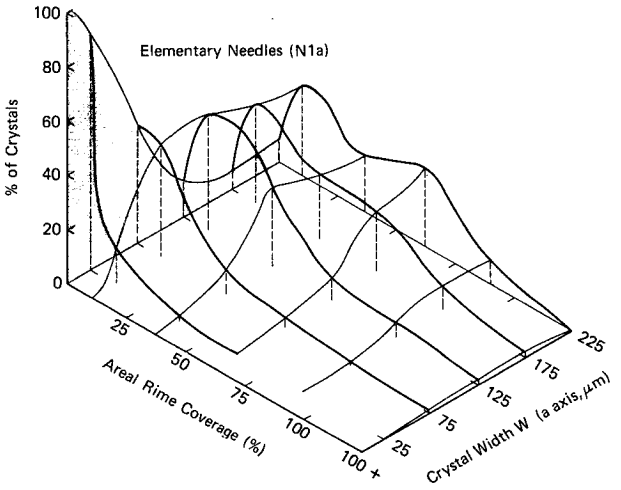

FIG. 3. Frequency distribution for elementary needles, in terms of crystal width.

Unauthenticated | Downloaded 05/21/24 01:11 AM UTC

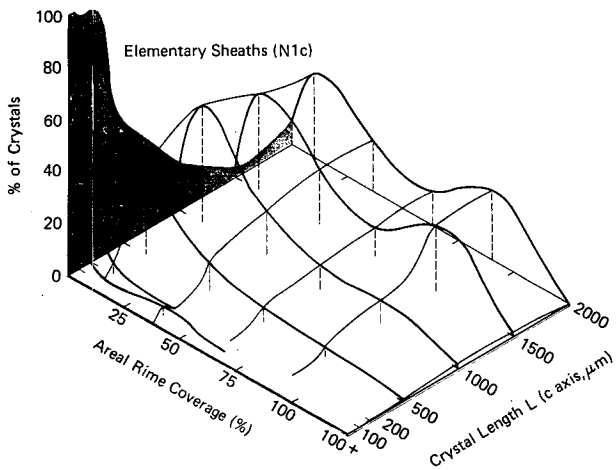

FIG. 4. Frequency distribution for elementary sheaths, in terms of crystal length.

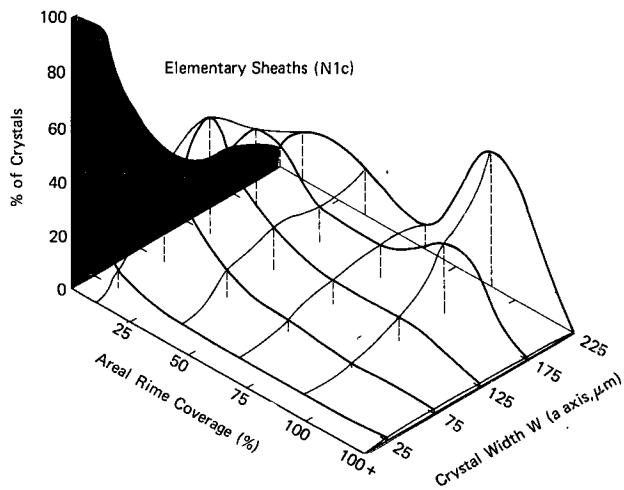

FIG. 5. Frequency distribution for elementary sheaths, in terms of crystal width.

and progression of accretion for the represented crystal populations; individual snow crystals were visually classified according to rime coverage on their main collecting surfaces by using a scale separating 1) unrimed crystals, and crystals with rime coverages of 2) 1–25%, 3) 25–50%, 4) 50–75%, 5) 75–100% and 6) graupel.

The zero rime category is clearly separated from the 1–25% category, so the onset of riming on individual crystals is readily resolved. An areal rime coverage of about 25% represents a somewhat arbitrary but suitable demarcation between insignificant and significant effects of riming on crystal shape, bulk density, aerodynamic behavior, and consequent rates of subsequent riming and any splinter production. Therefore, to examine the crystal transitions that describe the onset of riming and the initial buildup of significant accumulations of rime, the unrimed category and the 1–25% category of rime coverage are emphasized in this study, although the others are not to be ignored.

Three-dimensional (3-D) frequency distributions of the areal rime coverage were devised to graphically illustrate the sampled populations of the various planar and columnar crystals. Procedural details are given by Reinking (1973, 1975). The x, y, z coordinates, are respectively, crystal size, areal rime coverage and percentage of crystals. The surface defined by each 3-D distribution shows 1) the size distribution of crystals with any given rime coverage, 2) the dispersion and mode in the amounts of rime on the crystals of any given size, and 3) the trends of both the dispersion and the mode with increasing crystal size (or equivalent depositional growth time, assuming reasonable correlation between time and size).

Such 3-D frequency distributions for accretion on elementary needles and sheaths are shown in Figs. 2–5. To represent an opposite extreme in structural and riming complexity, the 3-D distribution for radiating crystals is shown in Fig. 6. Distributions for the following snow crystals and groups of crystals already have been presented by Reinking (1975): a composite of needles and sheaths, including bundles; hollow columns; a composite of needles, sheaths, columns and capped columns; hexagonal plates; and a composite of all branched planar crystals. Distributions for the structurally complicated and more erratically behaved broken branches and columns with hexagonal and dendritic caps are presented by Reinking (1973).

From these analyses, polynomial curves were computed to determine average rime coverage as a function of crystal type and size. Figs. 7 and 8, for elementary needles, are examples.

Root-mean-square (rms) errors for the curves define the dispersion of the means for the individual size intervals. The points in the graphs designated by triangles are mean values based on fewer than five crystals. These points were excluded in computation of the fitted curves.

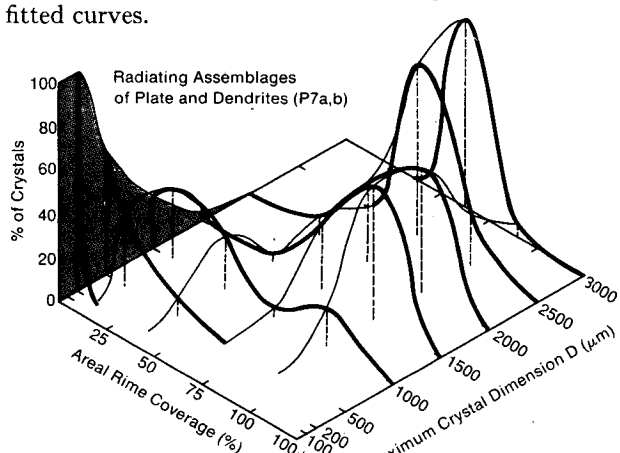

FIG. 6. Frequency distribution for radiating crystals, in terms of maximum crystal dimension. (Magono and Lee crystal types P7a and P7b are included here in group P2.)

Unauthenticated | Downloaded 05/21/24 01:11 AM UTC

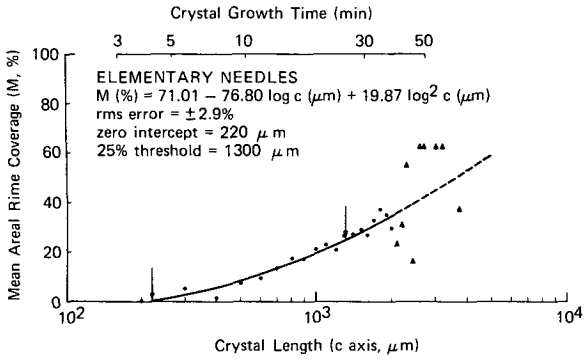

FIG. 7. Mean areal rime coverage M on elementary needles of length c and equivalent duration of crystal growth by deposition. In this and subsequent figures, the triangles represent mean values based on fewer than five crystals; these points were excluded in computation of the curves. Arrows indicate zero and 25% coverage.

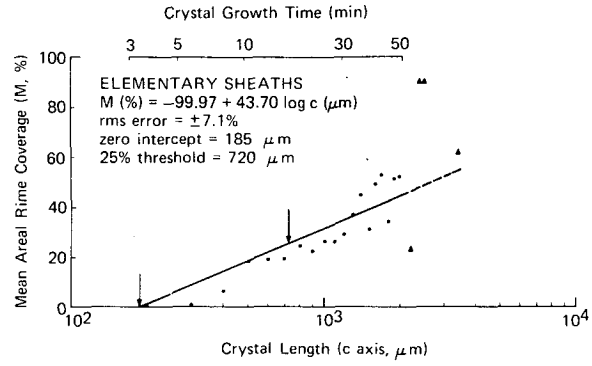

FIG. 9. As in Fig. 7, for elementary sheaths of length c.

Crystal growth times equivalent to the observed crystal sizes are included on these graphs as appropriate. The growth times for the various habits were computed using the temperature-dependent parameters for depositional growth rates at water saturation as given by Hindman and Johnson (1972). Growth times for the planar crystals are based on sizes of the "diameter" or a axis. Growth times for columnar crystals are based on crystal length or c axis.

Some procedural notes are warranted. Initially, columnar crystal growth times to the onset of accretion were separately estimated from the curves for the a and the c axes. The a and c axes maintain a proportional relationship for each specific columnar crystal habit, so theoretically the growth time could be based on either dimension. However, estimates based on the curves for the a axis, or width, were of the order of 1 min shorter than those based on the c axis. While in a practical sense this discrepancy in time is small, the estimates based on the analysis of the c axis are the most accurate. A certain absolute error in the measurement of columnar crystal length results in a lesser percentage error than the absolute error in the measurement of width. Given a measurement of size, the relatively rapid growth per unit time along the length axis allows for greater resolution in the determination of growth time. These factors are reflected in the smaller scatter of points and the consequent smaller rms error in mean rime for the curve fitted to the data on lengths. This is true of the needles, for example. Considering the natural scatter in c/a ratios for all types of columnar crystals, the minimum growth times to onset based on the crystal lengths are accurate to about ±1 min. The lengths of columnar crystals have been used to establish the growth times presented here.

The curves of mean rime coverage are most accurate, in relation to both crystal size and growth time, between the onset and the intermediate stages of accretion. Nonuniform buildups of rime, particularly on the planar crystals, probably led to numerical weighting of the curves that was too light to represent the heavier stages of rime. Therefore, if the larger percentages of mean areal rime coverage were translated into equivalent masses of rime, they would approximate the average lower limits of the accreted water.

Mean rime curves for elementary sheaths, hollow columns, hexagonal plates, branched planar crystals and radiating crystals are given in Figs. 9–15.

Sizes of droplets of rime were acquired by use of a method that was practical for the large sample of snow crystals. Diameters of one to five droplets were measured on each rimed crystal, when the rime was not so heavy as to make the sizes indistinguishable. The measured droplets were visually selected to represent the size range on each crystal. A size of 5 μm could be re-

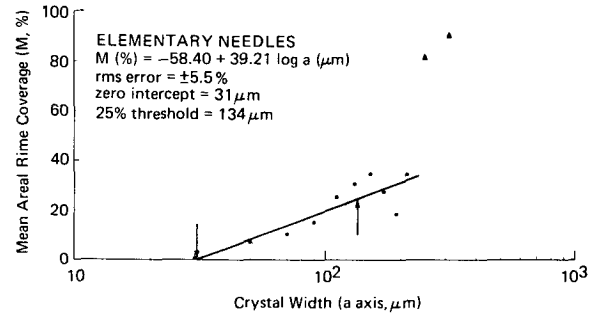

FIG. 8. Mean areal rime coverage M on elementary needles of width a.

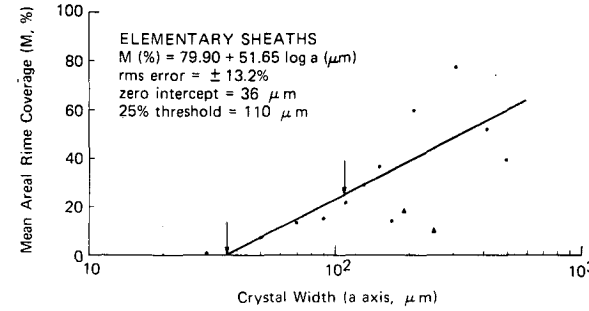

FIG. 10. As in Fig. 8, for elementary sheaths of width a.

Unauthenticated | Downloaded 05/21/24 01:11 AM UTC

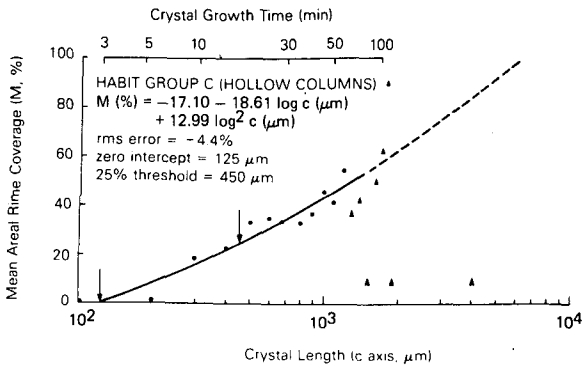

FIG. 11. As in Fig. 7, for hollow columns of length c.

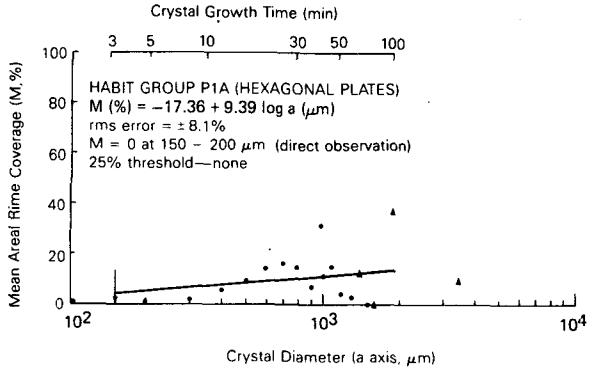

FIG. 13. As in Fig. 6, for hexagonal plates of major dimension a.

solved. From these measurements, an average size $\bar{d}$ of accreted droplets was estimated for each crystal. Each average diameter was recorded to the nearest 5 μm. The dispersion of diameters about any given average was normally about plus or minus one-third of the average value. This observation agrees with analyses of individual rime droplets made by Ono (1969), Wilkins and Auer (1970) and Kikuchi (1972). The shape of an accreted droplet is better represented by a hemisphere than a sphere (Brownscombe and Hallett, 1967); therefore, the measured diameters were assumed to represent hemispheres and were converted to equivalent diameters of spheres to estimate actual sizes of the accreted cloud droplets.

3. Accretion in terms of crystal population

Ice crystals originate from deposition nuclei, the freezing of small cloud droplets or from ice splinters ejected during a multiplication process, according to the model of Scott and Hobbs (1977). In any case, the maximum dimension of each new crystal is very small and normally too small to invite riming. Thus, by inference, in the 3-D distributions of observed rime amount (e.g., Figs. 2 and 3 for needle crystals), the beginning of growth of 100% of the crystals is represented by a point near (0,0,100). Take the distributions for the observed needle crystals as examples. As the needles grew, the accretion rate and the consequent rime coverage remained at or near zero until the c axis of individual crystals exceeded ~200 μm and the corresponding a axis exceeded ~25 μm. Continued depositional growth then led to accretion accelerating for more and more crystals. This can be noted in Figs. 2 and 3 as follows: First, consider the percentages of crystals with any given *small* size in each category of areal rime coverage; the percentages are at or near zero except in the no-rime category which contains most of the crystals. Next, note how the percentages of crystals that gain significant rime increase toward larger crystal sizes; as the collecting surfaces of more and more crystals become 25, 50 or 75% rimed, fewer and fewer crystals remain in the unrimed category. For example, only ~25% of the observed needles remained in the unrimed category upon growing to an approximate length of 1 mm and width of 90 μm. The fraction of the crystals of any size that have not encountered the onset of riming is represented by the shaded (x,z) plane in each of Figs. 2 and 3.

Examination of the shaded areas and the discussion of the observations thus far lead to two important conclusions:

1) Individual crystals must indeed reach some critical minimum size before measurable fractions of a population of snow crystals with a given habit will begin to rime.

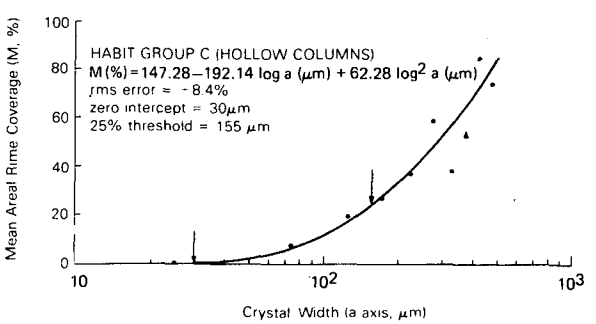

FIG. 12. As in Fig. 8, for hollow columns of width a.

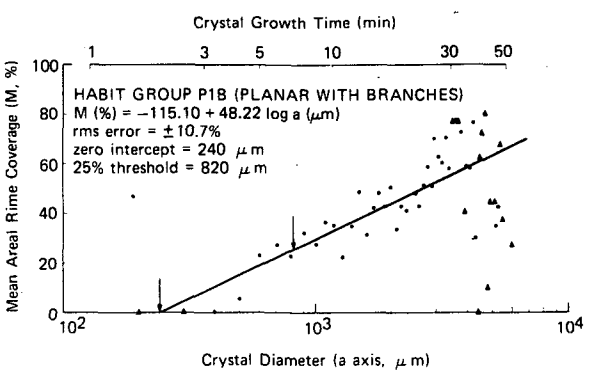

FIG. 14. As in Fig. 6, for branched planar crystals of major dimension a.

Unauthenticated | Downloaded 05/21/24 01:11 AM UTC

2) Many crystals in a given population do not begin to rime when the critical minimum size is reached. Rather, the onset of accretion is delayed over longer growth periods for large fractions of the crystal population, so considerable dispersion occurs in the actual sizes at onset. Indeed, a few crystals reach the maximum observed sizes without riming.

These conclusions apply to crystals with all types of growth habits, as shown by the observations in Figs. 2–6 and the referenced 3-D frequency distributions. Also, these conclusions apply for any given time during the observed snowstorms, as well as to the snowfall from the several storms considered collectively. None of the storms observed approached total glaciation, even temporarily. The predominance of snow crystals in the Sierra Nevada had growth habits that required water saturation or slight supersaturations to develop (see Magono and Lee, 1966); and a few of each habit grew to large sizes without riming. Questions could arise regarding the saturation levels responsible for the observed plates and columns. However, these crystals precipitated along with heavily rimed needles, sheaths and dendrites (Table 3, Reinking, 1975), so water saturation is definitely indicated.

The needles and sheaths grew within the lowest and warmest, supercooled cloud regime. Crystals of the minimum size for accretion and smaller could have grown within several tens of meters of the sampling site. A possible complication is that crystals grown so close to the ground might not rime under any circumstances due to lack of liquid water. However, cloud bases were still lower, and warmer than freezing, upwind and downslope from the sampling site. Thus, liquid water was continually replenished to the needle and sheath regime. As noted above, this replenishment was sufficient to maintain the water saturation required for the needle and sheath growth habits, so it must have been sufficient to maintain droplets. The reasons are good to assume that the smaller crystals had the opportunity to rime but did not because of their size.

Some further interpretations of all the 3-D distributions and some comparisons to theories and to other observations may now be made.

Field observations by Ono (1969) and Iwai (1973) suggest that all crystals of at least some habits, growing in mixed-phase clouds, will be rimed before reaching a certain size. Ono and Iwai empirically estimated that needles, sheaths and columns will collect rime before growing to a width (*a* axis) of 90–100 μm. However, in the Sierran sample, about 22, 33 and 37%, respectively, of the observed needles (Fig. 3), sheaths (Fig. 5) and columns of 100 μm width were still unrimed. Clearly, such a size limit cannot be assigned.

In natural clouds, *populations* of snow crystals compete for the droplets. While most crystals in the Sierran clouds will collect rime, a few crystals will, with high probability, grow for long times to large sizes without

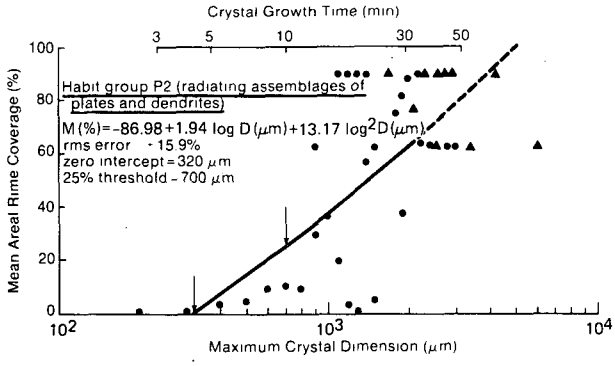

FIG. 15. As in Fig. 8, for radiating assemblages of plates and dendrites of major dimension *D*.

accreting. Convective clouds imbedded in more stratiform clouds are common over the Sierra Nevada in winter. The rates of accretion in the convective and stratiform volumes should not be expected to be the same. Conceivably, accretion could occur primarily in the convective cells where liquid water influx is greatest, while crystals formed or detrained into the stratiform volumes could grow mainly by deposition. Also, very small volumes of cloud might become depleted of droplets of accretable size by intense deposition on locally high concentrations of crystals. Spatial variations in the presence of droplets of accretable size on the microscale or imbedded-cumulus scale could logically introduce the observed wide ranges in crystal sizes at onset and in final degrees of riming on crystals of a population, as depicted by the 3-D distributions.

This concept of variable riming on populations of crystals which encounter variable microphysical and dynamical cloud conditions, as indicated by the observations, must be carried through to the theory. The onset of accretion is normally presumed to occur during the early stages of depositional growth of all crystals. This is easily, and incorrectly, inferred from some current theories and models that predict accretion will begin as soon as crystal growth leads to a nonzero efficiency for the collection of droplets with commonly occurring sizes (Hindman and Johnson, 1972; Pitter and Pruppacher, 1974; Schlamp *et al.*, 1975). These models treat only the growth of single crystals, and the uniform presence of droplets of accretable size is assumed. The more complex, but realistic, "quasi-stochastic" model of Scott and Hobbs (1977), for example, has begun to address this problem. In this model, continuous collection is assumed to occur on crystals after they begin to rime. This probably is not always true since some rimed crystals may enter cloud volumes where the droplet population is low or depleted (see Fig. 1). However, the quasi-stochastic description "allows for the simultaneous existence of both rimed and unrimed crystals of the same size and produces a broader distribution of rimed crystals" than would be obtained by starting accretion on all crystals

Unauthenticated | Downloaded 05/21/24 01:11 AM UTC

TABLE 1. Estimates of the onset and the 25% threshold of accretion.

CRYSTAL HABIT GROUP	(a) Major Crystal Dimension					(b) Crystal Width			(c) Cross-sectional Area	
	Crystal Dimension	Average Minimum Size at Onset (μm)	Average Minimum Growth Time at Onset (min)*	Average Size at 25% Rime Coverage (μm)	Average Growth Time at 25% Rime Coverage (min)	Crystal Dimension	Average Minimum Size at Onset (μm)	Average Size at 25% Rime Coverage (μm)	Average Minimum Area at Onset ($mm^2 \times 10^3$)	Average Area at 25% Rime Coverage ($mm^2 \times 10^3$)
N (Needlelike)	(L)	140	2.6	1100	25.0	(W)	34	120	4.8	132
N1a (Needles)	(c)	220	4.1	1300	25.0	(a)	31	134	6.8	174
N1c (Sheaths)	(c)	185	3.3	720	19.0	(a)	36	110	6.7	79
C (Columns)	(c)	125	3.1	450	17.0	(a)	30	155	3.8	70
P1A (Plates)	(a)	150	3.3	None	—	—	—	—	15.0	—
P1B (Branched Planar)	(a)	240	1.9	820	6.6	—	—	—	21.0	239
P1C (Broken Branches)	(L)	125	—	730	—	—	—	—	—	—
P2 (Radiating)	(D)	320	4.2	700	9.9	—	—	—	—	—
CP (Capped Columns)	(c)	115	2.7 (a)** 9.5 (b)	200	5.7 (a)** 29.0 (b)	(a of cap)	34	53	—	—

*Based on c axis for columnar types of crystals.
**For capped columns, growth time (a) corresponds to formation of a columnar part at −8C to −10 C, and (b) corresponds to formation at −20 C to −30 C.

reaching a set size. The Sierran observations presented above validate the need for approaches to modeling that account for variations in the degrees of riming on the crystals of whole populations.

4. Mean rime coverage

The average minimum crystal size and growth time at the onset of accretion may be specified from the observations for each principal growth habit by determining the average rime coverage as a function of crystal size and equivalent duration of growth. Average crystal sizes and growth times at stages of increasing rime load may also be defined in this way. The smallest and first crystals to collect rime are specified in each of Figs. 7–15 by the intercept of the curve with the abscissa.

a. Riming of columnar crystals

Rime is collected predominantly on the prism faces of the columnar types of crystals. Thus, the a and c axes define the approximately rectangular cross section presented to the airflow, as long as rime is light or uniform so the crystals do not tumble end-over-end or spiral. Estimates of sizes and growth times at the onset of riming for the basic columnar crystals are taken from Figs. 7–12 and are summarized in Table 1.

The observed columns, sheaths and needles grew to respective average minimum widths of 30, 36 and 31 μm and lengths of 125, 185 and 220 μm to reach the onset of riming. The respective average minimum durations of growth to onset were 3.1, 3.3 and 4.1 min. The growth rate used to determine growth time for the columns—habit group C—is based on crystal formation between −8 and −10°C. Most of the observed columns did form here, as is evident from the average length-to-width ratios which substantially exceed unity (e.g., from Figs. 10 and 11, at $M=25\%$, $c/a=450/155=2.9$). Columns that form between −20 and −30°C have c/a ratios near 1.2 (Auer and Veal, 1970; Hindman and Johnson, 1972). According to growth rates of the c axis given by Hindman and Johnson, the columns from relatively cold cloud would require a somewhat shorter time to attain the critical 30–35 μm dimension which would lead to riming if the same criterion applies when c/a is near unity.

The observed mean crystal length at the onset of riming for composite habit group N is less than those for either elementary needles or sheaths but the onset widths are about the same (Table 1). This may be explained by group weighting due to broader crystals. Group N includes primarily the elementary crystals, but also includes and is weighted by bundles and other structural combinations of needles and sheaths.

The uniformity of the observed widths of the various columnar crystals at riming onset indicates that the a axis is the most critical dimension in determining the onset of riming on columnar crystals. A corollary is that the average minimum duration of growth leading to onset of riming on columnar crystals is inversely

Unauthenticated | Downloaded 05/21/24 01:11 AM UTC

proportional to the growth rate of the a axis, and is influenced relatively little by the growth rates of the c axis or the consequent cross-sectional areas of the crystals. This is reflected in the three growth times of the columns, needles and sheaths, and more strongly in the respective lengths and areas (length-width products) for these crystals (Table 1). The bundles and combinations of needles and sheaths included in the composite group present wider or more irregular obstacles to airflows and thus collect cloud droplets somewhat more efficiently to produce the onset of riming at shorter lengths and apparently shorter equivalent growth times.

The onset of riming on columnar types of crystals has been studied theoretically and in other field situations by other investigators. Several comparisons are possible.

The field data presented by Ono (1969) and Iwai (1973) independently verify that the onset is most sensitive to the size of the a axis (width). However, their data indicate that droplets will begin to accrete on the columnar types of crystals only when widths exceed about 50 μm. Rimed columnar crystals narrower than 50 μm were observed in the Sierran snowfall; a few of these were more than 25% covered by rime. The average minimum onset widths of 30–36 μm determined from the Sierran observations can be allowed a tolerance up to ± 10 μm. The maximum positive adjustment would set the onset sizes at 40, 46 and 41 μm for columns, sheaths and needles, respectively. This adjustment does not eliminate the difference between present observations and those of Ono and Iwai, but does agree with recent observations of D'Errico and Auer (1978) who found an approximate threshold of 40 μm.

Physical causes of the size difference from the separate sets of observations are possible. In clouds containing small droplets (diameters <20 μm) with narrow size spectra, the ice crystals must grow by deposition to relatively large sizes in order for riming to commence (Pitter and Pruppacher, 1974). However, differences in the sizes of accretable cloud droplets apparently cannot account for the onset size difference. The rime droplets of the small sample measured by Ono (1969) ranged in diameter of equivalent spheres from about 12–55 μm, whereas those measured from the Sierran data (Fig. 16) and by D'Errico and Auer ranged from about 5–60 μm. Collection efficiencies of columnar crystals are initially the highest for droplets with diameters of 30 ± 10 μm, according to theory by Schlamp *et al.* (1975); droplet sizes within this range were heavily represented in all three samples.

The measurements of drop size in these cases neglect any growth of the frozen droplets on the crystals after collection. It is assumed that such growth would lead to crystalline edges that would obscure the hemispherical form of the droplets such that frozen droplets with significant growth would not be measured or counted.

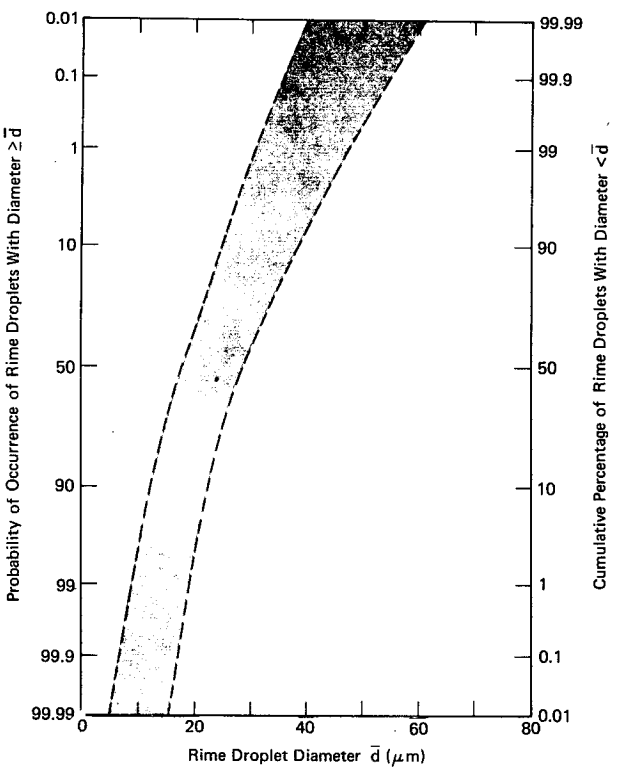

FIG. 16. Envelope (dashed lines) of individual cumulative size distributions of cloud droplets accreted on the various individual types of snow crystals.

The method of using curves of mean rime coverage to estimate the average minimum crystal sizes and growth times at the onset of riming may have an advantage over establishing a rime/no-rime demarcation by the method of Ono and Iwai. A field sample of snow crystals, however large in a practical sense, is still a minute fraction of all the crystals that precipitate. Thus, a size demarcation, like the 50 μm crystal width determined on an absolute rime or no-rime basis without considering the *trend* in amounts of rime versus crystal size, may well shift from sample to sample. This may well explain the difference between previous and present estimates of the critical size. The larger the total sample, the more crystals there will be in the tail of the distribution that represents the onset of accretion. The method of using the mean rime curve establishes an onset that is based not just on the demarcation separating unrimed and rimed crystals of the sample, but also on the whole trend of rime coverage increasing with crystal size from the onset to heavy stages. A smooth continuity is thus established between the onset and the accumulations of rime that follow. Thus, the tail of the distribution is more reliably accounted for, and the critical dimensions so determined are likely to be more representative of the true minimum sizes at the onset.

Schlamp *et al.* (1975) theorized that the onset of riming on columns will occur when the a axis grows to

Unauthenticated | Downloaded 05/21/24 01:11 AM UTC

some dimension between 47.0 and 65.4 μm, as the collection efficiency increases from zero to ~20%. Scott and Hobbs (1977), with the aid of collection efficiencies from Schlamp *et al.*, model growth of the columnar types of crystals so that a width of 67 μm is required for the onset of riming. These sizes also exceed the 30–40 μm critical width for columnar crystals determined here. Schlamp *et al.* used the most up-to-date theories of collection efficiencies available, although even these might be improved, perhaps by the addition of electrical effects (Pitter, personal communication).

Accretion rates in the crystal growth model of Hindman and Johnson (1972) are estimated from collection efficiencies determined by Ranz and Wong (1952). These efficiencies as applied to snow crystals are generally excessive and very approximate since snow crystals predominantly have Reynolds numbers considerably less than 100 so the incorporated theory for potential flow is not justified (Reinking, 1973; Pitter and Pruppacher, 1974). Predictions of the columnar crystal riming from the Hindman and Johnson model are most readily compared to the present data for needles. The model computations for crystal growth at −5°C indicate that needles will begin to rime at widths of 32.5 μm. Curiously, despite the dubious collection efficiencies, this estimate is in excellent agreement with the 31 μm width found from the Sierran observations.

We now consider the measurements of accretion beyond the onset and to the 25% "threshold" of mean areal rime coverage. The significance of this degree of riming was explained earlier.

The Sierran data strongly contradict the conclusion of Ono (1969) that riming of needles and sheaths "is very rare because their minor axes [remain] below the riming limit;" needles and sheaths rimed to and beyond the 25% stage of coverage were observed in profusion during the Sierran snowstorms, as shown by Figs. 2–5 and 7–10.

Crystal sizes at the 25% threshold are included in Table 1. The widths of the observed columnar types at this threshold are again comparable, in view of the increasing scatter of the data with increasing crystal size. The durations of growth to this stage are also comparable, with the observed sequence of minor differences in time still holding true. The columns reached this stage first, followed in order by the sheaths and needles.

Theories and other observations show that the bulk densities are, respectively, smaller for columns, sheaths and needles (Hindman and Johnson, 1972; Ryan *et al.*, 1976), and the terminal velocities of these crystals vary directly with the densities. The efficiencies for collecting droplets vary directly with the crystal fallspeeds, relative to the droplet fallspeeds, so the observed pattern in the growth times to the 25% stage is logically explained.

b. Ice splintering and the copious presence of needles and sheaths

Laboratory evidence first discussed by Hallett and Mossop (1974) indicates that secondary ice particles will be generated when ice crystals in natural clouds collect rime under limited physical conditions. This "splinter" production is confined to the −4° to −8°C temperature regime in which crystals develop predominantly by the needle and sheath habits of growth, requires abundant cloud droplets with diameters exceeding about 24 μm, and also requires that the relative velocities of colliding ice particles and droplets exceed ~0.7 m s^{-1}. Concentrations of needles and sheaths exceeded 10 ℓ^{-1} during many of the observed precipitation episodes, whereas the worldwide average ice nucleus spectrum would predict 10^{-2} ℓ^{-1} at most (Reinking, 1975). The observed profusion of needles and sheaths may have resulted from the cloud seeding in most cases. However, these crystals precipitated in an average concentration of 5.5 ℓ^{-1} during one *non-seeded* storm [episode 25, Table 3, Reinking (1975)]. An analysis of this "needle anomaly" has been presented by Reinking (1978). Suffice it to say in summary that, within the Sierran cloud systems, the −4 to −8°C temperatures occurred regularly, roughly 50% of the droplets collected as rime are estimated to have been larger than the critical 24 μm size (Fig. 16), and rimed ice particles or crystal aggregates with fallspeeds great enough to meet the relative velocity restriction fell through the −4 to −8°C regime and precipitated with the needles and sheaths. Some abnormal crystal generating process was active; certainly splinters from accreting droplets could have induced large crystal concentrations in both the seeded and unseeded cases.

Note that the relative velocity requirement is not met by individual needles and sheaths of sizes observed (Bashkirova and Pershina, 1964; Heymsfield, 1972; Reinking, 1973). This aspect of the splintering mechanism has been somewhat neglected.

c. Riming of planar and radiating crystals

Rime on a planar crystal is collected primarily on the basal face that encounters the air stream. This face is represented by the *a* axis. Radiating assemblages of plates and dendrites (P7a,b in the Magono and Lee classification, combined in group P2 here) are roughly spherically symmetric, so they are represented by their diameters *D*. The average minimum sizes at the onset of riming on the branched planar crystals (240 μm) and the radiating crystals (320 μm) are the largest observed (Figs. 14 and 15, Table 1, habit groups P1B and P2). The branched planar crystals form in the cloud regime of most rapid depositional growth (−15±3°C), and the radiating types of crystals fall into this regime to attain most of their size after forming at colder temperatures. The consequent average minimum growth time to onset for the observed branched planar

Unauthenticated | Downloaded 05/21/24 01:11 AM UTC

crystals is very short (1.9 min). Hindman and Johnson (1972) predict that snow crystals growing at −15°C will encounter the onset of riming within 1–2 min, which equates to a size between 150 and 300 μm; the Sierran data show good agreement with a time and size near the greater of these.

The radiating crystals begin to form at relatively cold temperatures as they must grow slowly and settle for some time before reaching the regime of rapid growth; thus their growth time to onset is longer. The 4.2 min estimated for these crystals from the Sierran sample (Table 1) is physically reasonable but very approximate.

Habit group P1C in Table 1 represents branches broken from planar crystals. The average minimum size of these observed crystal fragments at the onset of riming is only slightly greater than half the size of the whole branched planar crystals at the onset. The data *suggest* that crystal fracturing occurs simultaneously with or shortly after the onset of riming. A physical connection of the two processes could be implied.

The axial growth rate of hexagonal plates is less than one-third that of the branched planar crystals (Hindman and Johnson, 1972), so the growth time to the observed onset of riming is longer for the plates (3.3 min vs 1.9 min). However, the size of the plates at the onset of riming is somewhat less than that of the branched crystals (150–200 μm vs 240 μm); this difference is also reflected in the respective cross-sectional areas at onset (Table 1c). The mean rime curve for plates (Fig. 13) was not a good fit; the lack of a clear riming pattern as a function of plate size is not explained. The given range for onset size was determined by direct observation of the individual plates, rather than from the fitted line. However, Harimaya (1975) worked with a substantial sample to find a plate onset size of 150 μm, very close to that found here. Also, measurements by Wilkins and Auer (1970) reveal a minimum onset size of ~200 μm for plates. The sample used to determine this size was extremely small so this size cannot be regarded as an absolute minimum; however, data from a subsequent study in the same location indicated a threshold of 140 μm (D'Errico and Auer, 1978). From another small sample, Ono (1969) suggested that riming is rare on plates with $a<300$ μm. All of the data except Ono's clearly show that 140–200 μm plates will rime; albeit, as shown by the Sierran crystals, relatively small percentages of the plates collect significant amounts of rime [Fig. 13; and Fig. 3 in Reinking (1975)].

The most up-to-date theoretical estimates of accretion efficiencies for plates have been calculated by Pitter and Pruppacher (1974) and revised by Pitter (1977). They find that the efficiency begins to exceed zero and plates begin to rime only when the a axis grows to a size within the 294–320 μm range. The model of Scott and Hobbs (1977) requires plates to grow to 364 μm before riming is allowed to occur. These estimates are too large, as the observations of natural crystals show.

Given these analyses of the riming onset, we now consider the observed planar and radiating crystals as they accreted to the 25% threshold of rime coverage. The effect of the rapid growth of branched planar crystals and radiating crystals on droplet collection after the onset of riming is evident in the growth times required to reach the 25% threshold (Table 1). The respective total growth times of only 7–10 min may be compared to the 17–25 min required by the basic columnar types to accumulate the same coverage on their collecting surfaces. The hexagonal plates grew by deposition to diameters as large as 1500 μm. However, after 3 or 4 min of growth, the areas of the droplet-collecting faces of branched planar crystals exceed those of plates with similar growth times by more than an order of magnitude. Thus, it is not surprising that the observed plates did not, in the mean, accumulate sufficient rime to cover 25% of their surfaces (Table 1). The observations show that *the branched planar and radiating crystals accumulate water by accretion at rates much faster than those for all the other types of crystals, with the possible exception of capped columns which begin growth in clouds at −8 to −10°C* (see below).

d. Riming of capped columns

Accurate estimation of the riming characteristics of capped columns was complicated by the complex shapes and generally heavy accumulations of rime on the observed crystals. Combined data for plate-capped and dendrite-capped columns indicate that the columnar sections must reach an average minimum length of roughly 115 μm to start to accrete droplets. The caps only slightly exceed the widths of the columnar sections at this time.

Caps would normally be expected to form on columns that nucleate between −20 and −30°C and then settle down to warmer regimes where the planar habits develop. However, the c/a size ratios of the observed columnar sections are greater than expected within reasonable growth times at these cold temperatures. The ratios are in much better accord with growth rates of columns forming between −8 and −10°C. Growth times for both possibilities are presented in Table 1. Imbedded convection could have carried warm zone columns up to the −10 to −20°C regime for planar cap growth; the 2.7 min time to onset is regarded as the best estimate.

At the 25% threshold of rime coverage, the measured mean c axes of the capped columns are substantially smaller than the c axes of the ordinary columns. Consequently, the caps, however small, do definitely and profoundly increase the efficiency for collection of droplets. However, the total concentrations of capped columns are generally less than those of the other types

Unauthenticated | Downloaded 05/21/24 01:11 AM UTC

of crystals so relatively small portions of the total precipitated water is carried by capped columns.

5. Conclusions

The observations confirm that individual snow crystals must grow by deposition to at least a critical minimum size before they can begin to collect cloud droplets. The observations also show that many of the crystals comprising a population in a mixed-phase cloud grow well beyond the critical minimum size before they begin to rime; this is apparently a result of the stochastic nature of accretion, the competition among crystals for cloud water, and nonuniform spatial distributions of droplets of accretable size even in clouds that on the average contain large quantities of liquid water. Empirical estimates and theoretical models that depict the onset of accretion only on crystals of small size do not describe all the crystals that rime in a given cloud system. The models need to account for the whole distribution of crystal sizes at the onset of riming, as shown, for example, in Figs. 2–6. The model of Scott and Hobbs (1977) makes a significant stride in this direction. It incorporates a quasi-stochastic formulation that allows for the simultaneous existence of both unrimed and rimed crystals of the same size, and it produces a broader, more realistic distribution of rimed crystals than would be obtained by continuous accretion from the minimum onset sizes.

The critical minimum sizes of snow crystals at the onset of accretion are reported above as averages for the basic growth habits from the Sierran snow sample. The observational estimates show that minimum lengths or diameters of crystals within the approximate range of 115–320 μm have to be attained before any crystals will begin to rime. The widths of columnar types of crystals must grow to a minimum of 30–36 μm ± 10 μm; the onset of riming on these crystals is regulated primarily by this dimension with little influence from the lengths or cross-sectional areas.

The critical minimum sizes of specific types of crystals determined from the Sierran field sample are somewhat less than those observed by Ono (1969) and Iwai (1973), and those predicted by the theories of Pitter and Pruppacher (1974), Schlamp *et al.* (1975) and Pitter (1977). However, they are comparable to those observed by Wilkins and Auer (1970), Harimaya (1975) and D'Errico and Auer (1978), and those predicted by Hindman and Johnson (1972). Curiously, the Hindman and Johnson model of accretion has the least rigid theoretical basis. Some improvement of the theoretical accuracies is apparently still warranted.

The average minimum durations of depositional crystal growth prior to riming are estimated from the Sierran sample to be between 1.9 and 4.2 min and are thus quite similar for all crystal types. However, the observations show systematic variations with crystal habits in both the growth times and the minimum sizes required for riming. Columns, sheaths and needles, with respectively lesser bulk densities, do respectively grow to larger minimum lengths and require longer minimum times to reach the onset of accretion. Bundles and other combinations of needles and sheaths are broader collectors so they reach the critical size sooner than single needles and sheaths. Branched planar crystals grow to minimum droplet collecting sizes in relatively short times. Hexagonal plates must grow for longer times, but to lesser sizes than the branched crystals.

The relative differences observed among the various basic crystal types at the onset of riming are carried through to at least the stage when 25% of the collecting surfaces of the crystals become covered with rime. However, the average capped columns have only small caps and follow the minimum size characteristics of ordinary columns at the rime onset, but develop much accelerated accretion rates as the caps grow and 25% rime coverage is approached.

Roughly at the 25% stage, the effects of riming on aerodynamics (fallspeed, fluttering, tumbling, etc.) of all crystals begin to significantly affect further growth, and accretion becomes a major contributor to total precipitation. The average trends of observed riming to and beyond the 25% stage show that the branched planar and radiating crystals and the capped columns develop the most significant rates of accretion and precipitate the greatest masses of water in the form of rime. Theories and models need to account quite specifically for riming differences among the individual, basic types of crystals, so as to more accurately account for differences in the masses of water precipitated. The model of Young (1974) addresses this problem but the most appropriate accretion efficiencies are not used and the model does not allow for the statistically distributed nature of the onset and progression of accretion.

Secondary ice particles from accreting droplets may contribute significantly to the very large populations of needles and sheaths observed in the Sierran snowstorms. The proper temperatures occur regularly along with the required, relatively large super-cooled droplets. The requirement that the relative velocities of colliding crystals and droplets must exceed 0.7 m s^{-1} to induce splintering (Hallet and Mossop, 1974) can also be met in the Sierran cloud systems, but apparently not by individual needles and sheaths, which settle slowly; this restriction deserves more attention and investigation.

Acknowledgments. The roots of the paper were part of a Ph.D. dissertation written for Colorado State University and supported by the California State Department of Water Resources under Agreement B-50882, the U.S. Bureau of Reclamation under Contract 14-06-D-6592, and the Naval Weapons Center. Professor Lewis O. Grant and Dr. Pierre St.-Amand are particularly acknowledged for their support. This paper is dedicated to the memory of Tom Wehan who dili-

Unauthenticated | Downloaded 05/21/24 01:11 AM UTC

gently assisted in the collection and reduction of the data.

REFERENCES

Auer, A. H., and D. L. Veal, 1970: The dimensions of ice crystals in natural clouds. *J. Atmos. Sci.*, **27**, 919–926.

Bashkirova, G. M., and T. A. Pershina, 1964: On the mass of snow crystals and their fall velocity. *Tr. Gi. GeoFiz. Observ.*, **156**, 83–100.

Brownscombe, J. L., and J. Hallett, 1967: Experimental and field studies of precipitation particles formed by the freezing of supercooled water. *Quart. J. Roy. Meteor. Soc.*, **93**, 455–473.

D'Errico, R. E., and A. H. Auer, 1978: An observational study of the accretional properties of ice crystals of simple geometric shapes. *Preprints Conf. Cloud Physics and Atmospheric Electricity*, Issaquah, Amer. Meteor. Soc., 114–121.

Hallett, J., and S. C. Mossop, 1974: Production of secondary ice particles during riming process. *Nature*, **249**, 26–27.

Harimaya, T., 1975: The riming properties of snow crystals. *J. Meteor. Soc. Japan*, **53**, 384–392.

Heymsfield, A., 1972: Ice crystal terminal velocities. *J. Atmos. Sci.*, **29**, 1348–1357.

Hindman, E. E., II, and D. B. Johnson, 1972: Numerical simulation of ice particle growth in a cloud of supercooled water droplets. *J. Atmos. Sci.*, **29**, 1313–1321.

Iwai, K., 1973: On the characteristic features of snow crystals developed along *c*-axis. *J. Meteor. Soc. Japan*, **51**, 458–465.

Jiusto, J. E., and R. L. Lavoie, 1975: AMS symposium on the prediction and measurements of ice crystal concentrations in clouds (summary). *Bull. Amer. Meteor. Soc.*, **56**, 1175–1179.

Kikuchi, K., 1972: On snow crystals with small raindrops. *J. Meteor. Soc. Japan*, **50**, 142–144.

Magono, C., and C. W. Lee, 1966: Meteorological classification of natural snow crystals. *J. Fac. Sci. Hokkaido Univ.*, Ser. 7, **2**, 321–335.

Mason, B. J., 1975: Production of ice crystals by riming in slightly supercooled clouds. *Quart. J. Roy. Meteor. Soc.*, **101**, 675–679.

Ono, A., 1969: The shape and riming properties of ice crystals in natural clouds. *J. Atmos. Sci.*, **26**, 138–147.

Pitter, R. L., 1977: A re-examination of riming on thin ice plates. *J. Atmos. Sci.*, **34**, 684–685.

——, and H. R. Pruppacher, 1974: A numerical investigation of collision efficiencies of simple ice plates colliding with supercooled water droplets. *J. Atmos. Sci.*, **31**, 551–559.

Ranz, W. E., and J. B. Wong, 1952: Impaction of dust and smoke particles. *Ind. Eng. Chem.*, **44**, 1371–1380.

Reinking, R. F., 1973: Empirical assessment of accretion microphysics. Ph.D. dissertation, Colorado State University, 342 pp.

——, 1975: Formation of graupel. *J. Appl. Meteor.*, **14**, 745–754.

——, 1978: The needle anomaly in Sierra Nevada snowfall. *Preprints Conf. Cloud Physics and Atmospheric Electricity*, Issaquah, Amer. Meteor. Soc., 247–252.

Ryan, B. F., E. R. Wishart and D. E. Shaw, 1976: The growth rates and densities of ice crystals between −3°C and −21°C. *J. Atmos. Sci.*, **33**, 842–850.

Schlamp, R. J., H. R. Pruppacher and A. E. Hamilec, 1975: A numerical investigation of the efficiency with which simple columnar ice crystals collide with supercooled water droplets. *J. Atmos. Sci.*, **32**, 2330–2337.

Scott, B. C., and P. V. Hobbs, 1977: A theoretical study of the evolution of mixed-phase cumulus clouds. *J. Atmos. Sci.*, **34**, 812–826.

Wilkins, R. I., and A. H. Auer, 1970: Riming properties of hexagonal ice crystals. *Preprints Conf. Clouds Physics*, Ft. Collins, Amer. Meteor. Soc., 81–82.

Young, K. C., 1974: A numerical simulation of wintertime, orographic precipitation: Part I. Description of the model microphysics. *J. Atmos. Sci.*, **31**, 1735–1748.

Unauthenticated | Downloaded 05/21/24 01:11 AM UTC